

## A theoretical study about three organic semiconductor based on oligothiophenes

Yarui Shi, and Huiling Wei\*

*College of Physics and Electronic Engineering, Henan Normal University, Xinxiang 453007, China*

Received 10 July 2015; Accepted (in revised version) 15 August 2015

Published Online 30 September 2015

---

**Abstract.** Three derivatives based on oligothiophenes were theoretically investigated about the electronic and charge transport properties using density functional (DFT) theory based on the Marcus-Hush theory. The predicted highest hole mobility is  $0.218 \text{ cm}^2\text{V}^{-1}\text{s}^{-1}$ , and the highest electron mobility is 0.373 at 300 K. The calculated data demonstrated that the compound 1 should be a high-performance n-type organic material candidate and compound 3 may well be potential p-type materials with high mobility values. Our work also indicates that the face-to-face  $\pi$ - $\pi$  interaction and S-S interactions is favorable for the molecular stacking and charge transport behaviors. The calculated results provide an additional possibility to be able to improve the origin semiconductor performance and design new electronic devices.

**PACS:** 81.05.Fb, 78.40.Me

**Key words:** Organic semiconductor, charge transport, Oligothiophene.

---

### 1 Introduction

Organic semiconductor materials are promising materials for organic field effect transistors (OFETs), organic light emitting diodes (OLEDs), and organic photovoltaic cells (OPVCs) because of their potential applications in low-cost, flexibility, and mass chemical synthesis during the past decades. [1-7] Many efforts have been exclusively conducted to improving the performances of the organic semiconductor, such as designing new organic semiconductors and optimizing device configurations. As we all know, the performance of the semiconductors depends largely on the charge transport. [8-10] It is crucial to understand the principles of charge transport and the relationship between the performance and the electronic structure for the material structure design.

---

\*Corresponding author. *Email address:* syrwuli@163.com (H. L. Wei)

Thiophenes-based materials are an important class of organic semiconductors because they exhibit many different intra- and intermolecular interactions from the high polarizability of S electrons in the thiophene rings. [11-15] Oligothiophenes are among the most effective molecular for organic materials with significantly electronic properties. Furthermore, the organic device shows remarkable charge carrier mobility in OFETs, as high as  $2.0 \text{ cm}^2\text{V}^{-1}\text{s}^{-1}$  based on annelated  $\beta$ -oligothiophenes. [16] S-S and S- $\pi$  intermolecular interaction can provide different charge transport pathways. It is very necessary to a further study of the relationship between the interactions and the performance. Recently, organic semiconductors have been widely investigated based on  $\beta$ -oligothiophenes. To further investigate the relationship of electron property and structure for the thiophene-based materials, discussions of the charge transport properties are studied based on three single crystal structures.

In this work, we investigate Charge transport behavior is of great interest in organic materials. The performance of the devices strongly depends on their charge transport, quantified by the charge-carrier mobility. Room-temperature mobility for many different single-organic molecules have been reported. We need to gain a complete theoretical fundamental understanding of the mobility in organic materials to understand the structure-transport relationships and transport mechanisms, and the theoretical method

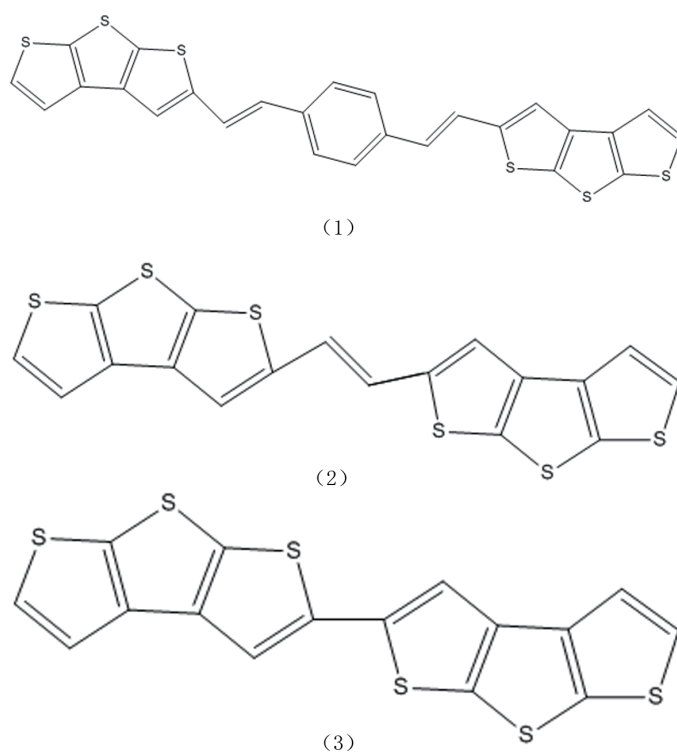


Figure 1: Molecular structure of compounds 1-3.

is independent of the measurement techniques and sample preparation to eventually predict the mobility from the first-principles DFT calculations. Charge mobility can be expressed many types, such as the thermally averaged velocity-velocity tensor and the charge effective mass tensor. Indeed, many research groups have investigated the electron transport to describe organic semiconductors by using Marcus theory.

## 2 Theory and methods

### 2.1 Evaluation of the reorganization energy

The reorganization energy  $\lambda$  is usually divided into two types: the *internal* and *external* reorganization contributions ( $\lambda_1$  and  $\lambda_2$ ). [17, 18]

$$\lambda = \lambda_1 + \lambda_2. \quad (1)$$

The former is related to the change of the donor and acceptor sites consecutive to the gain or loss in equilibrium geometry during electron-transfer process, and the latter dominates the energy change of the electronic and nuclear polarization (relaxation) in the biological environments. External reorganization energy has small contribution in condensed-state systems, so the external contribution is neglected in many practices. The reorganization energy  $\lambda$  calculation formulae can be written as follows

$$\lambda = \lambda_1 = \lambda_{rel}^1 + \lambda_{rel}^2 = [E^0(G^\pm) - E^0(G^0)] + [E^\pm(G^0) - E^\pm(G^\pm)]. \quad (2)$$

$\lambda_{rel}^1$  corresponds to the relaxation energy from the stable geometry of the ionic state to the lowest energy geometry of one neutral molecule, and  $\lambda_{rel}^2$  corresponds to the relaxation energy of the reverse process. Where  $E^\pm(G^\pm)$  and  $E^0(G^0)$  are the energies of optimized geometry of neutral and charged state,  $E^\pm(G^0)$  are charged energies of the optimized neutral geometry, and the  $E^0(G^\pm)$  are the neutral energies of charged state respectively. At the same time, we evaluate the adiabatic ionization potential (IP) and electron affinities (EA) by the following equations

$$IP = E^+(G^+) - E^0(G^0) \quad (3)$$

$$EA = E^-(G^-) - E^0(G^0). \quad (4)$$

### 2.2 Evaluation of the intermolecular effective electronic coupling

The electronic coupling  $V$  is based on the different molecular orbitals of the conjugated molecules. In the following the intermolecular effective electronic coupling  $V_{ij}$  can be calculated directly by the following equation.

$$V_{ij} = \left| \frac{J_{ij} - S_{ij}(e_i + e_j)/2}{1 - S_{ij}^2} \right|. \quad (5)$$

Where the site energies ( $e_i, e_j$ ), charge-transfer integrals ( $J_{ij}$ ), and spatial overlap ( $S_{ij}$ ) can be calculated from  $e_i = \langle \psi_i | H | \psi_i \rangle$  ( $e_j = \langle \psi_j | H | \psi_j \rangle$ ),  $J_{ij} = \langle \psi_i | H | \psi_j \rangle$  and  $S_{ij} = \langle \psi_i | \psi_j \rangle$ .

### 2.3 Theoretical models

In recently years, many different models have been proposed linking molecular properties to charge carrier mobility, such as the coherent band model and the incoherent hopping model. The charge transfer between adjacent molecules occurs via the hopping process. However a macroscopic charge transport requires a large number of incoherent hopping processes. In our article, the charge carrier mobility  $\mu$  can be expressed by the Einstein-Smonluchowski equation

$$\mu = \frac{e}{k_B T} D. \quad (6)$$

Where  $\mu$  is the mobility,  $e$  is the electronic charge,  $k_B$  is Boltzmann constants, and  $T$  is the temperature respectively.  $D$  is the isotropic charge diffusion coefficient which is related to the charge transfer rate constant  $W$  as summing over all possible hopping pathways in the crystal. The diffusion coefficient  $D$  can be given by the equation from the hopping rates as

$$D = \frac{1}{2n} \sum_i r_i^2 W_i P_i. \quad (7)$$

Where  $n=3$  is the spatial dimensionality,  $i$  is the specific pathway with the distance to neighbor  $i$   $r_i$ ,  $W_i$  is the hopping rate due to charge carrier to the neighbor, and  $P_i = W_i / \sum_i W_i$  is the hopping probability for the  $i$ th hopping pathway. The charge transfer rate constant  $W$  can be described as follow from Marcus-Hush theory. [18-21]

$$W = \frac{V^2}{\hbar} \left( \frac{\pi}{\lambda k_B T} \right)^{1/2} \exp\left(-\frac{\lambda}{4k_B T}\right). \quad (8)$$

In recent years, a useful model has been developed to calculate the anisotropic mobility by Han and his partners. They project the electronic coupling pathway of different dimer types onto the transport channel relative to the reference axis of the molecular crystal [22].

$$\mu_\phi = \frac{e}{2k_B T} \sum_i r_i^2 W_i P_i \cos^2 \gamma_i \cos^2(\theta_i - \phi). \quad (9)$$

$\gamma_i$  is the angle of the hopping jumps between adjacent molecules relative to the plane of interest (in our article  $\gamma_i$  are  $0^\circ$ ),  $r_i$  is the hopping distance, and  $\theta_i - \phi$  is the angle between the pathways and conducting channel respectively.

#### 2.3.1 Computational details

As we all known, we can use the density functional theory (DFT) to calculate electronic properties and molecular configuration of organic semiconductor compounds. Through text it is found that the 6-31G(d) basis set combining with the B3LYP functional can give

Table 1: The calculated Molecular Frontier Orbital Energies (HOMO and LUMO), Energy gaps (H-L gap), IPs, and EAs) with unit eV.

molecule	HOMO	LUMO	H-L gap	IP	EA
1	-5.36391	-2.41093	2.952981	-1.45412	6.28625
2	-5.13125	-1.76275	3.368499	-0.59204	6.232273
3	-5.37724	-1.36764	4.0096	-0.19429	6.493086

the closest prediction values compared with experimental values in the calculation of the many energy-related properties such as frontier molecular orbital energies. The electronic coupling is computed using TA2P basis set with PW91 gradient corrections, which shown to provide the best result in the Amsterdam density functional (ADF) program.

All quantum chemistry calculations can be carried out with the Gaussian09 program package and the Amsterdam density functional (ADF) program. [23,24]

### 3 Results and discussion

To our knowledge, the frontier orbital energies are important for understanding the charge-transfer property, so the calculated Molecular Frontier Orbital Energies (highest occupied molecular orbital (HOMO) and lowest unoccupied molecular orbital (LUMO)), ionization potentials (IPs), electron affinities (EAs) and HOMO-LUMO energy gaps are compared. The energies are listed in Table 1.

The HOMO levels of compounds 1 and 3 are estimated to be similar values (-5.364 eV for compound 1 and -5.377 eV for compound 3), which are much lower than that of compound 2 (-5.131 eV). However, compound 3 displays a high-lying LUMO energy of -1.368 eV and the highest HOMO-LUMO gap of 4.009 eV. In contrast to compound 3, compound 1 shows a low-lying LUMO energy of -2.411 eV and the lowest HOMO-LUMO gap of 2.953 eV. These results show that compound 1 possesses a lower electron injection barrier than the other molecules as n-type organic semiconductor materials. The EA energies are important property determining the performance for example the device durability. Among three compounds, the compound 3 exhibits a very large EA value of 6.493 eV, which indicates compound 3 is expected to be a quite air-stable materials.

As seen in Fig. 2, most of the electrons are localized over the planar framework on the carbon atom. The extended  $\pi$ -conjugated systems in LUMO imply that the compound 1 and 2 are promising n-type organic semiconductors. The HOMO have a broader conjugated system than LUMO for compound 3, that is to say, the compound 3 may be better p-type organic materials candidates than p-type materials. The calculated results of reorganization energies  $\lambda_h$  and  $\lambda_e$  are listed in Table 2. We notice that the energies  $\lambda$  are almost equal for hole and electron transfer of compound 1-3. Furthermore, the compound 1 exhibits relatively small  $\lambda$  values, which suggest that compound 1 should function as a more high efficiency candidates than compounds 2 and 3.

Table 2: The calculated reorganization energies  $\lambda$  (eV) in compound 1-3.

molecule	1	2	3
Hole transfer $\lambda_h$	0.252288	0.30793	0.372679
Electron transfer $\lambda_e$	0.242802	0.292547	0.37909

Table 3: The calculated hole (electronic) coupling  $V$  (in meV) and the intermolecular center-of-mass distances (in Å) for different possible hopping passways

	1			2			3		
	Vh	Ve	r	Vh	Ve	r	Vh	Ve	r
P	2.672	31.664	5.920	10.949	18.703	5.742	2.3915	5.6689	6.273
T1	32.132	66.267	4.797	36.618	61.623	4.772	66.893	40.428	3.789
T2	32.132	66.267	4.797	36.618	61.623	4.772	8.1526	10.348	5.267

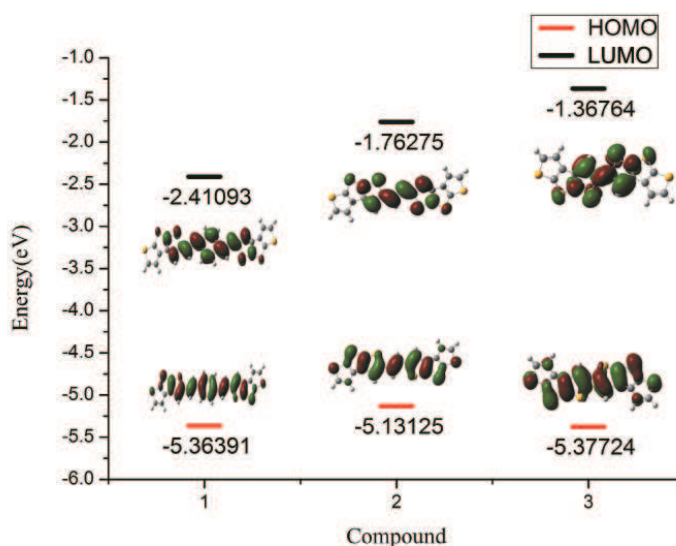
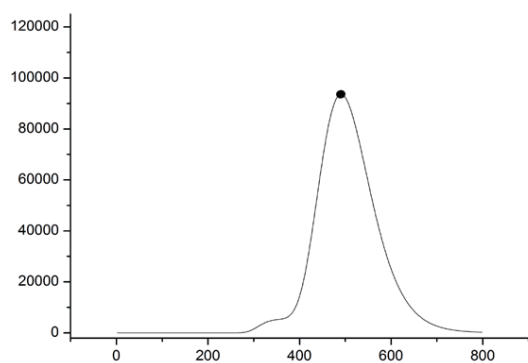


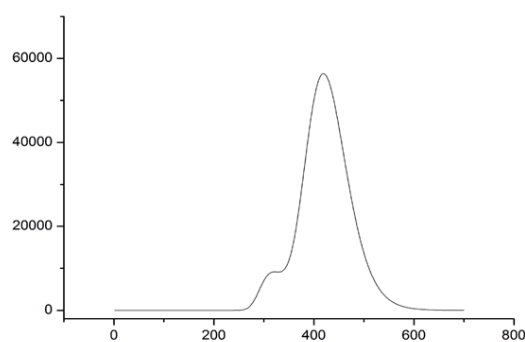
Figure 2: Frontier molecular orbitals of optimized compounds 1-3.

Fig. 3 shows the simulated absorption spectra of compound 1-3. We can note: the predicted maximum absorption peaks are 491, 418, and 386 nm, respectively. In addition, it is seen that there are slightly red-shift  $386(3) < 418(2) < 491(1)$  nm, corresponding to the  $\pi$ - $\pi^*$  transition and the absorption of the aryl group.

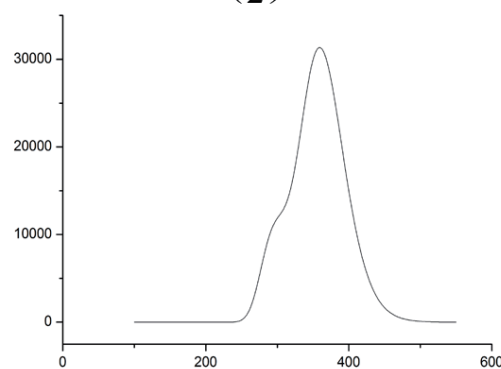
To evaluate the charge transport mobility, the intermolecular charge-hopping coupling  $V$  is one critical parameter of the capability for materials. The effective charge transfer integrals and the center-mass distances for all possible hopping passways are listed in Table 3. As shown, the largest charge transfer integrals are 66.893 meV for hole transfer of compound 3 and 66.267 meV for electron transfer of compound 1, respectively. In addition, the largest  $V$  is much smaller than the calculated reorganization energies



(1)



(2)



(3)

Figure 3: UV-visible absorption spectra of compound 1-3.

(0.373 and 0.243 eV), so we can be sure that the calculation of the charge transfer mobility is adequate based on the semiclassical Marcus-Hush theory. The  $V$  values are really different in different hopping pathways. It can be noted that the T ways can provide the

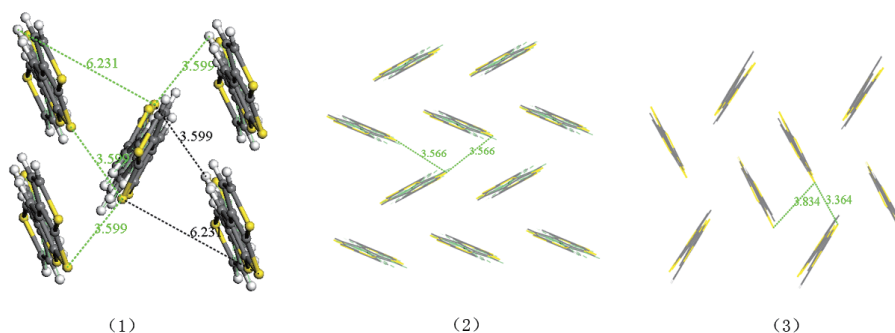


Figure 4: S-S intermolecular interactions in the single crystal structures of compounds 1-3.

largest charge-transfer integral because of the face-to-face stacking and the shortest distance. The largest hole transfer integrals for compound 1-3 are 32.132, 36.618, and 66.893 meV at pathway T. Meanwhile the largest electron transfer integrals are 66.267, 61.263, 40.428 meV for compound 1-3. The T packings have shorter distance compared with other dimers, such as 4.797, 4.772, and 3.798 Å, respectively. As we all know, the face-to-face stacking means a large degree of the interacting orbital overlap. It is very interesting that there are three different intermolecular interactions from S-S to S- $\pi$ , which can improve the device performances. As shown in Fig. 4, various S-S intermolecular interactions with shortest distances of 3.599, 3.568, and 3.834 Å for compound 1-3, respectively. The existence of the larger S-S intermolecular interaction will cause the smaller  $\pi$ - $\pi$  spacing, and the edge-to-face  $\pi$ - $\pi$  interactions are expected to provide other packing pathway for charge transport.

The charge transport mobility  $\mu$  is calculated based on the efficiency parameters, such as the computed  $\lambda$  and  $V$ , with the Marcus-Hush theory in this work. The predicted highest hole mobility are 0.08727, 0.06468, and 0.09119  $\text{cm}^2\text{V}^{-1}\text{s}^{-1}$  at 300 K for compound 1-3 respectively. Moreover the calculated highest electron mobility of 1-3 is 0.37361, 0.21777, and 0.02902  $\text{cm}^2\text{V}^{-1}\text{s}^{-1}$  respectively. These results indicate that the compounds 1 and 2 may be potential candidate for electron transport material.

The compound 1-3 have remarkably anisotropic mobility behavior as seen in Figs. 5-7, which show the predicted anisotropic mobility curves in the single crystals 1-3. The largest hole and electron mobility are near  $88^\circ/268^\circ$ ,  $93^\circ/273^\circ$ , and  $54^\circ/224^\circ$  in the angle-resolution figure, which are 0.087 and 0.373  $\text{cm}^2\text{V}^{-1}\text{s}^{-1}$  for compound 1, 0.218 and 0.065  $\text{cm}^2\text{V}^{-1}\text{s}^{-1}$  for compound 2, and 0.029 and 0.091  $\text{cm}^2\text{V}^{-1}\text{s}^{-1}$  for compound 3.

## 4 Conclusions

In summary, three novel semiconductor based ontrithiophenes have been theoretically investigated by the first-principle DFT level based on the Marcus-Hush theory. Through



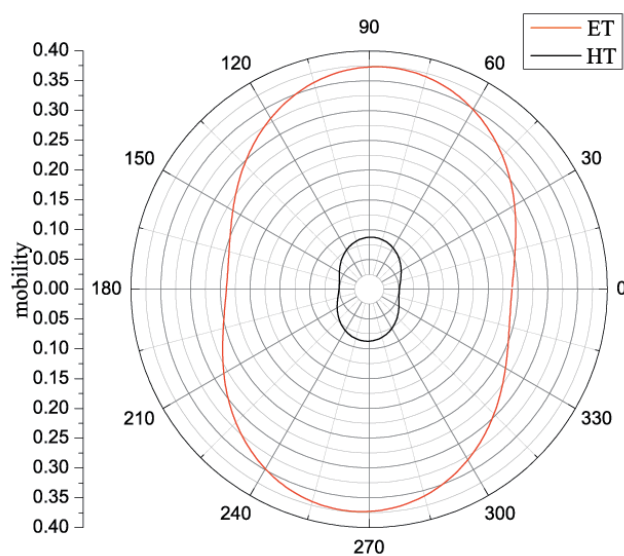


Figure 5: Predicted anisotropic mobility curves of compound 1 (in  $\text{cm}^2\text{V}^{-1}\text{s}^{-1}$ ).

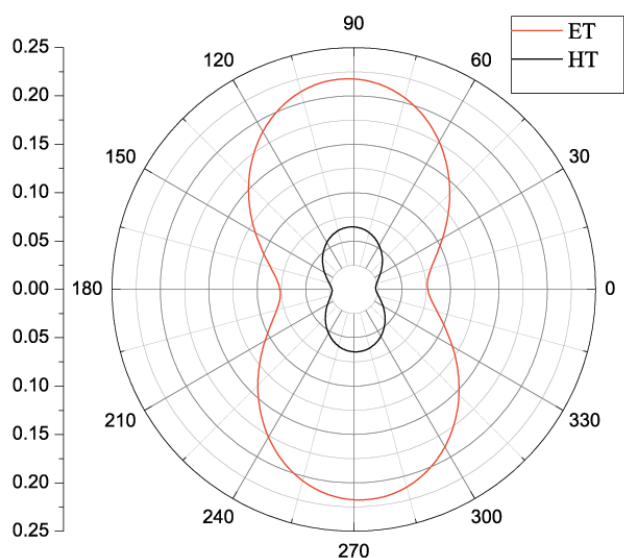


Figure 6: Predicted anisotropic mobility curves of compound 2 (in  $\text{cm}^2\text{V}^{-1}\text{s}^{-1}$ ).

the computation results (reorganization energies, charge transfer integrals, and the frontier orbital characteristics), they exhibit excellent performance with hole mobility up to  $0.218 \text{ cm}^2\text{V}^{-1}\text{s}^{-1}$  for compound 2 and electron mobility up to  $0.373 \text{ cm}^2\text{V}^{-1}\text{s}^{-1}$  for compound 1. The compound 1 and 2 may be promising candidates for n-type organic materials. However, compound 3 should be more favor to function as high-performance hole transport organic semiconductor. The packing mode, which combing face-to-face  $\pi$ - $\pi$  interactions and S-S interactions, is helpful for the charge transport behaviors. We

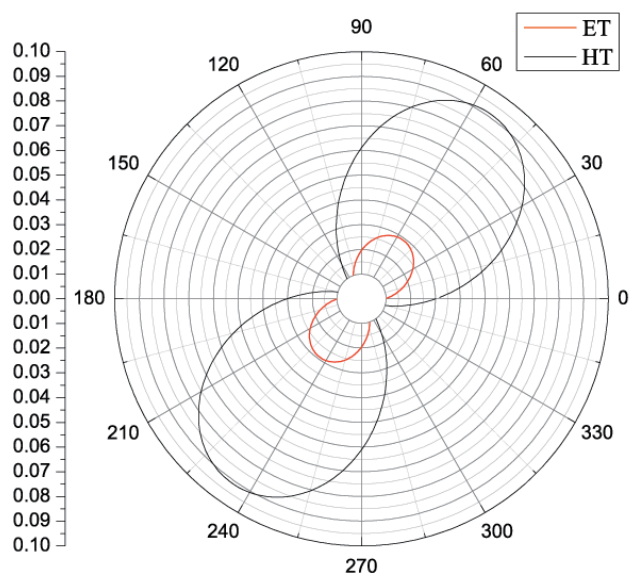


Figure 7: Predicted anisotropic mobility curves of compound 3 (in  $\text{cm}^2\text{V}^{-1}\text{s}^{-1}$ ).

can get better understand the charge transport property from the distribution of angular resolution anisotropic mobility.

**Acknowledgments.** This work was supported by the National Natural Science Foundation of China (Grant No. 11274096), Innovation Scientists and Technicians Troop Construction Projects of Henan Province of China (Grant No. 124200510013) and Science and Technology Research Key Project of Education Department of Henan Province of China (Grant No. 13A140690).

## References

- [1] C. Y. Chuang, P. I. Shih, C. H. Chien, F. I. Wu, C. F. Shu, *Macromolecules*, 40 (2007) 247.
- [2] S. R. Forrest, *Nature*, 428 (2004) 911.
- [3] S. O. Jeon, K. S. Yook, J. Y. Lee, *Thin. Solid. Films.* 519 (2010) 890.
- [4] J. H. Lee, P. S. Wang, H. D. Park, C. I. Wu, J. J. Kim, *Org. Electron.*, 12 (2011) 1763.
- [5] Y. Tao, Q. Wang, C. Yang, Q. Wang, Z. Zhang, T. Zou, J. Qin, D. Ma, *Angew. Chem. Int. Edit.*, 47 (2008) 8104.
- [6] Z. Wang, C. Kim, A. Facchetti, T. J. Marks, *J. Am. Chem. Soc.*, 129 (2007) 13362.
- [7] F. C. Wu, H. L. Cheng, C. H. Yen, J. W. Lin, S. J. Liu, W. Y. Chou, F. C. Tang, *Phys. Chem. Chem. Phys.*, 12 (2010) 2098.
- [8] S. Mohakud, S. K. Pati, *J. Mater. Chem.*, 19 (2009) 4356.
- [9] M. L. Tang, T. Okamoto, Z. Bao, *J. Am. Chem. Soc.*, 128 (2006) 16002.
- [10] Y. Yamaguchi, T. Ochi, S. Miyamura, T. Tanaka, S. Kobayashi, T. Wakamiya, Y. Matsubara, Z. Yoshida, *J. Am. Chem. Soc.*, 128 (2006) 4504.
- [11] M. Makoto, R. Andrzej, P. Maren, R. Suchada, *J. Am. Chem. Soc.*, 127 (2005) 13806.
- [12] A. Rajca, H. Wang, M. Pink, S. Rajca, *Angew. Chem. Int. Edit.*, 112 (2000) 4655.

- [13] W. Shao, H. Dong, L. Jiang, W. Hu, *Chem. Sci.*, 2 (2011) 590.
- [14] W. R. Silveira, E. M. Muller, T. N. Ng, D. Dunlap, J. A. Marohn, *Scanning Probe Microscopy* (2007).
- [15] X. Zhang, A. P. C00té, A. J. Matzger, *J. am. chem. soc* (2005).
- [16] L. Tan, L. Zhang, X. Jiang, X. Yang, L. Wang, Z. Wang, L. Li, W. Hu, Z. Shuai, L. Li, *Adv. Funct. Mater.*,19 (2009) 272.
- [17] G. R. Hutchison, M. A. Ratner, T. J. Marks, *J. Am. Chem. Soc.*, 127 (2005) 2339.
- [18] N. S F, B. F, *J. org. chem* 66 (2001) 6551.
- [19] J. Jortner, *J. Chem. Phys.*, 64 (1976) 4860.
- [20] M. Y. Kuo, C. C. Liu, *J. Phys. Chem.C.*, 113 (2009) 16303.
- [21] R. A. Marcus, *J. Chem. Phys.*, 43 (1965) 679.
- [22] Y. Shi, H. Wei, Y. Liu, *J. Mol. Struct.*, 1083 (2015) 65.
- [23] C. Fonseca Guerra, J. G. Snijders, G. te Velde and E. J. Baerends, Towards an order-N DFT method, *Theor. Chem. Acc.*, 99 (1998) 391.
- [24] G. te Velde, F. M. Bickelhaupt, S. J. A. van Gisbergen, C. Fonseca Guerra, E. J. Baerends, J. G. Snijders, T. Ziegler, *J. Comput. Chem.*, 22 (2001) 931.